The Biaxial Strain Dependence of J_C of a (RE)BCO Coated Conductor at 77 K in Low Fields

Jack R. Greenwood, Elizabeth Surrey, and Damian P. Hampshire

***Abstract*—Recently, we designed and commissioned a "cross-board" sample holder that can apply biaxial strains in the plane of a (RE)BCO coated conductor. It allows us to measure the critical current density J_C for arbitrary combinations of *x*- and *y*-strain. Understanding the in-field, in-plane, biaxial strain dependence of a tape's $J_C(B, \varepsilon_{xx}, \varepsilon_{yy})$ is crucial for applications such as CORC or Roebel cables, as the cables are subjected to multiaxial strains during manufacturing and operation. Here, we present experimental data for $J_C(B, \varepsilon_{xx}, \varepsilon_{yy})$ on a SuperPower SCS4050 APC tape in magnetic fields up to 0.7 T, at 77 K. We also outline a theoretical model for the biaxial strain dependence of J_C and use it to parameterize our data and show that the fraction of A-domains and B-domains are roughly equal ($f = 0.49 \pm 0.03$) and that the strain sensitivity of the critical temperature is 1.8 ± 0.1 K%$^{-1}$ and -1.3 ± 0.1 K%$^{-1}$ along their *a*- and *b*-axes, respectively, for all the domains in this (RE)BCO tape. For the first time, we show both parabolic and linear strain dependencies of J_C in a single tape by changing the angle between the applied strain direction and the twin boundaries in the (RE)BCO layer.**

***Index Terms*—Critical current, strain measurement, 2G HTS conductors, cuprates.**

I. Introduction

THERE are many applications of (RE)BCO coated conductors (commonly known as (RE)BCO tapes) in which the tapes are subjected to multiaxial loads during manufacturing and operation. For example, the (RE)BCO tapes in 'conductor on round core' (CORC) cables, which are constructed from tapes wound helically around a round core [1], are subjected to axial, transverse, and shear strains [2]. Roebel cables are also subjected to these strains, due to the material discontinuities across the widths of the cables [3]. Finite element models of CORC or Roebel cables under strain can be used to predict their electrical performance completely if the effect of strain on the critical current density (J_C) is comprehensively understood for an arbitrary strain direction (i.e., in three dimensions) [3], [4]. Therefore, there is a need to develop experimental equipment and mathematical models to measure and explain the multiaxial strain dependence of J_C, as this will allow cable manufacturers to optimise their cable designs to minimise the suppression of J_C with strain.

The effect on J_C by uniaxial strain along the length of a (RE)BCO tape is well known [5]–[12]. It has led to the tapes in CORC cables being wound at 45° to minimise the suppression of J_C with that type of strain [1], [5]. However, there have been comparatively fewer studies on the effect of the other types of strain on J_C [3], [13]–[16] and even fewer on the effect of having strains along multiple axes of a tape simultaneously [13], [16]. Single crystal data suggest that the in-plane strain dependence of the critical temperature T_C (and of J_C) is large (along the *a*-axis and *b*-axis) but very weak along the *c*-axis of (RE)BCO [17]. This means that biaxial measurements and understanding may provide a very significant improvement in our ability to predict the performance of these tapes in advanced applications with complex strain distributions. To this end, we have recently designed and commissioned a biaxial sample holder known as a 'crossboard' which can apply in-plane, biaxial strains to a tape [16]. The crossboard allows us to measure the in-plane biaxial strain dependence of J_C for arbitrary *x*- and *y*-strains (where the *x*-axis is parallel with the length of the tape and the *y*-axis is orthogonal to the length of the tape). The crossboard is manufactured from Berylco 25 and has *x*-strain and *y*-strain limits of $-0.50\% \leq \varepsilon_{xx} \leq 0.50\%$ and $-0.20\% \leq \varepsilon_{yy} \leq 0.15\%$ respectively.

In this paper, in Section II we present $J_C(B, \varepsilon_{xx}, \varepsilon_{yy})$ measurements as a function of *x*-strain and *y*-strain using the crossboard at 77 K in magnetic fields B up to 0.7 T. We then present the Biaxial Strain model for J_C (BSJ) and parameterise our results in Section III. The model considers (RE)BCO layer as a 1D chain of (RE)BCO A- and B-domains which have their *a*- and *b*-axes aligned with the length direction of the tape respectively. The in-field, in-plane, biaxial strain dependence of a whole tape's critical current density, $J_C(B, \varepsilon_{xx}, \varepsilon_{yy})$, is governed by the $J_C(B, \varepsilon_{xx}, \varepsilon_{yy})$'s of the A- and B-domains. The model and experimental results are then discussed in Section IV and then the paper concludes in Section V.

II. Experiments

A. Experimental Procedure

$J_C(B, \varepsilon_{xx}, \varepsilon_{yy})$ d.c. current transport measurements have been performed on a single SuperPower SCS4050 APC tape

Manuscript received October 30, 2018; accepted February 5, 2019. Date of publication February 8, 2019; date of current version March 29, 2019. This work was supported the by EPSRC Grant [EP/L01663X/1] for the Fusion Centre for Doctoral Training. This work has been carried out within the framework of the EUROfusion Consortium, funded by the Euratom research and training program 2014-2018 under Grant 633053. *(Corresponding author: Jack R. Greenwood.)*

J. R. Greenwood and D. P. Hampshire are with the Department of Physics, Superconductivity Group, Durham University, Durham DH1 3LE, U.K. (e-mail: jack.r.greenwood@durham.ac.uk; d.p.hampshire@durham.ac.uk).

E. Surrey is with the European Atomic Energy Community/Culham Center for Fusion Energy Fusion Association, Culham Science Center, Abingdon OX14 3DB, U.K.

Color versions of one or more of the figures in this paper are available online at http://ieeexplore.ieee.org.

Digital Object Identifier 10.1109/TASC.2019.2898343

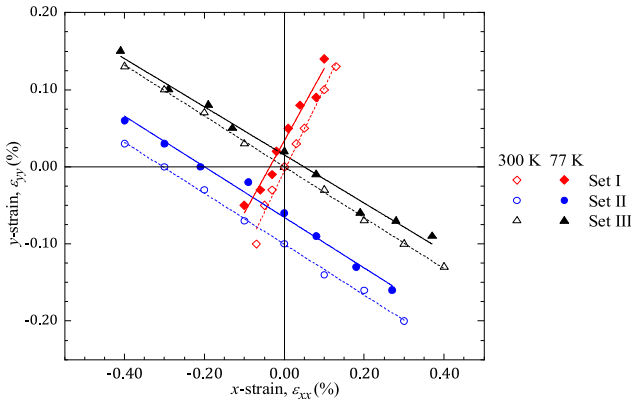

Fig. 1. The strains that were applied to the (RE)BCO tape. The open data points and dashed linear fits correspond to the strains that the tape were fixed to at 300 K and solid linear fits and closed data points correspond to the strains at 77 K.

sample in fields up to 0.7 T with the current density J orthogonal to the field at 77 K, with the field aligned parallel to the plane of the tape ($\theta = 0°$) and with it perpendicular to the plane of the tape ($\theta = 90°$). The tape's Hastelloy substrate is $\sim$50 μm thick and its (RE)BCO layer is $\sim$1 μm thick and contains artificial pinning centers (APC's). The shape and dimensions of the crossboard on which the sample is mounted have been described previously [16]. Put simply, the crossboard is a sample holder for the tape that is shaped like a cross. The pairs of opposite arms of the cross can be used to apply either tensile or compressive strains in orthogonal directions. The (RE)BCO tape sample had a width of 4 mm, a length of 24 mm and it was soldered with its substrate side facing downwards onto the center of a crossboard. A pair of voltage taps with a separation of 9 mm were soldered about the center of the tape. We have used the convention that the length of the tape was aligned with the x-axis of the crossboard. The strains ε_{xx} and ε_{yy} were measured using a HBM 1-XY91-1.5/120 2D T-rosette strain-gauge [18], which was glued onto the upper surface of the tape. The strain state of the tape was noted at room temperature before it was cooled to 77 K.

B. J_C Results

Fig. 1 shows the strains that were measured in this paper. At room temperature a strain was applied in each of both directions and the strains noted. The sample was then cooled to 77 K and the strain was noted again. J_C was then measured at 77 K every 0.1 T up to 0.7 T with J orthogonal to the field and with the field applied either parallel or orthogonal to the surface of the tape. An electric field criterion of 100 μVm^{-1} was used to calculate J_C. The sample was then warmed up to 300 K so the strain state of the tape could be changed. Three sets of strain data were obtained at 77 K and at room temperature as shown in Fig. 1. Table I gives the free parameter values of the linear fits to the strain values for each set of data. The error on the strains in Figs. 1–4 is $\Delta\varepsilon_{xx} \approx \Delta\varepsilon_{yy} \approx 0.02\%$ and is dominated by the uncertainty of the resistance of the strain gauge at zero strain. The free parameters and their errors were

TABLE I
FREE PARAMETER VALUES FROM THE LINEAR FITS IN FIG. 1

Strain Dataset	Temperature (K)	$\frac{\partial \varepsilon_{yy}}{\partial \varepsilon_{xx}}$	$\varepsilon_{yy}(\varepsilon_{xx} = 0)$ (%)
Dataset I	300	1.03±0.02	-0.002 ± 0.001
	77	0.94±0.01	0.034 ± 0.006
Dataset II	300	-0.330±0.007	-0.100 ± 0.002
	77	-0.33±0.02	-0.066 ± 0.004
Dataset III	300	-0.330±0.007	0.000 ± 0.001
	77	-0.31±0.01	0.015 ± 0.003

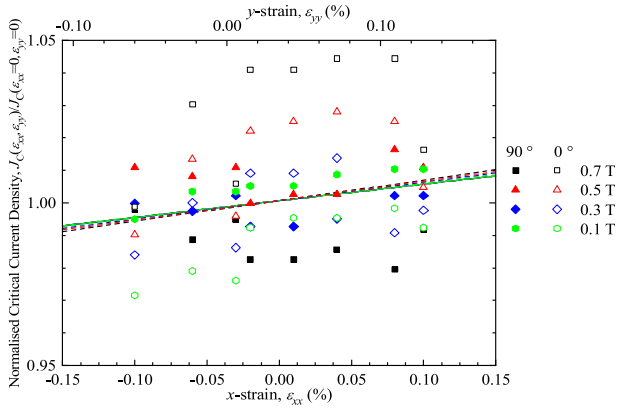

Fig. 2. The normalised critical current density as a function of x- and y-strain at 77 K for Dataset I. ε_{xx} is the independent variable and the ε_{yy} coordinates are calculated from the linear fit in Fig. 1. The dashed lines are fits to the $\theta = 0°$ data and the solid lines are fits to the $\theta = 90°$ data.

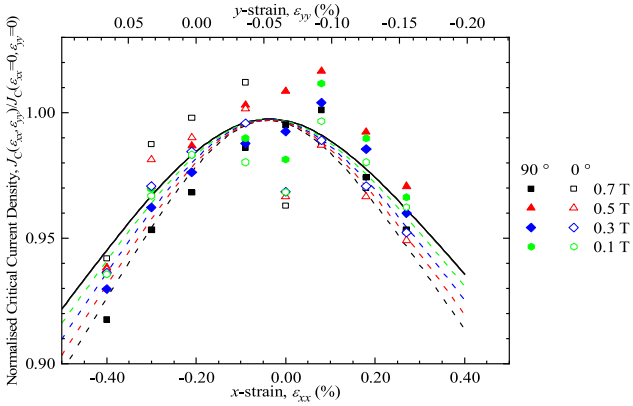

Fig. 3. The normalised critical current density as a function of x- and y-strain at 77 K for Dataset II. ε_{xx} is the independent variable and the ε_{yy} coordinates are calculated from the linear fit in Fig. 1. The dashed lines are fits to the $\theta = 0°$ data and the solid lines are fits to the $\theta = 90°$ data.

calculated by performing least-squares straight-line fits on each of the strain data sets. The associated sets of J_C data are shown in Figs. 2–4. In Fig. 2 strains were applied so that the x-strain and y-strain were the same (which we refer to as Dataset I). In Fig. 3, the crossboard was first strained along the y-axis, then different strains were applied along the x-axis (referred to as Dataset II). In Fig. 4, strains were applied along the x-axis only (which we refer to as Dataset III). J_C was measured as a function of field once at each of the strains in Dataset I first, followed by

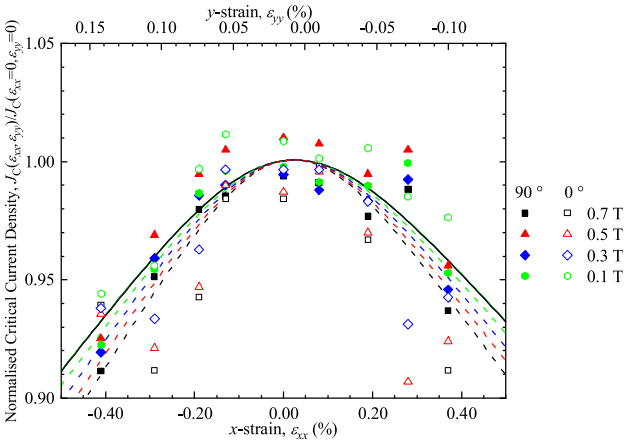

Fig. 4. The normalised critical current density as a function of x- and y-strain at 77 K for Dataset III. ε_{xx} is the independent variable and the ε_{yy} coordinates are calculated from the linear fit in Fig. 1. The dashed lines are fits to the $\theta = 0°$ data and the solid lines are fits to the $\theta = 90°$ data.

once for each strain in Dataset II and then once for each strain in Dataset III. Figs. 2–4 show data for fields every 0.2 T from 0.1 T up to 0.7 T, although data was obtained for 0.2 T, 0.4 T and 0.6 T as well. To ensure that J_C was reversible over the experimental strain range, $J_C(B, \varepsilon_{xx} = 0, \varepsilon_{yy} = 0)$ was measured between Datasets. There was no permanent degradation of $J_C(B, \varepsilon_{xx} = 0, \varepsilon_{yy} = 0)$ over the course of the experiment. Dataset I's J_C data in Fig. 2 is linear with respect to x-strain around $\varepsilon_{xx} = 0\%$. In contrast, Dataset II's and Dataset III's J_C data have parabolic behaviour with respect to applied x-strain around $\varepsilon_{xx} = 0\%$.

III. Theory and Parameterisation

Here we outline a straightforward biaxial strain model for these (RE)BCO tapes that extends the one-dimensional models in the literature [5], [6], [10]. We assume the superconducting layer can be represented by a 1D chain of A- and B-domains that have their crystallographic a- and b-axes aligned with the length direction of the tape respectively. The standard convention is that the Cu-O chains lie along the b-direction. In single crystals uniaxial tension along the a-direction increases T_C. The critical current density of the tape, J_C, can be calculated by considering the electric field contributions from each of the A- and B-domains. This leads to:

$$J_C = \left[f {J_{C,A}}^{-N} + (1-f) {J_{C,B}}^{-N} \right]^{-\frac{1}{N}}, \quad (1)$$

where f and $(1-f)$ are the fractions of A- and B-domains, $J_{C,A}$ and $J_{C,B}$ are the critical current densities of the A- and B-domains and N is the tape's quality index in each ith domain which is defined using the well-known $E-J$ power law

$$\frac{E_i}{E_C} = \left(\frac{J}{J_{Ci}} \right)^N, \quad (2)$$

where E_C is the electric field criterion usually taken to be 10 or 100 μVm^{-1}, E_i is the electric field and i is A or B. J_{Ci} of domain type i can be calculated using the engineering scaling law [6], [19]–[23]

$$J_{C,i} = A[B_{c2,i}]^{n-3} b^{p-1} (1-b)^q T_{C,i}^2 \left(1-t^2\right)^2. \quad (3)$$

The parameters A, p, q and n are fitting constants, $B_{c2,i}$ is the upper critical magnetic field of domain type i, b is the reduced field $B/B_{c2,i}$, $T_{C,i}$ is the critical temperature of domain type i and t is the reduced temperature $T/T_{C,i}$. In this paper n was set at 2.5 [24], [25], $B_{c2}(0,\ 0, 0)$ at 98.7 T for $\theta = 90°$ and 185 T for $\theta = 0°$ [6], [26] and $T_C(0,0)$ was set at 90.1 K [26], [27]. The critical temperature in domain type i is parameterised using the upper critical field where [6], [20], [21]:

$$\frac{B_{c2,i}\left(T, \varepsilon_{xx}, \varepsilon_{yy}\right)}{B_{c2}\left(0,0,0\right)} = \left(\frac{T_{C,i}\left(\varepsilon_{xx}, \varepsilon_{yy}\right)}{T_C\left(0,0\right)} \right)^w (1-t)^s, \quad (4)$$

where $B_{c2}(0,0,0)$ is the upper critical magnetic field of an A- or B-domain at zero temperature and zero strain and w and s are fitting constants. Here we have set w at 2.2 [6], [20] and s at 1.26 [6] to constrain the fits to data. Measurements of the uniaxial strain dependence of T_C of single crystals of (RE)BCO have shown that T_C varies linearly with planar strain [17], [27], [28]. Hence, we define the biaxial strain dependencies of $T_{C,A}$ and $T_{C,B}$ using:

$$\begin{aligned} T_{C,A}\left(\varepsilon_{xx}, \varepsilon_{yy}\right) &= T_C(0,0)(1 + g_A\left(\varepsilon_{xx} - \varepsilon_{xx0}\right) \\ &\quad + g_B(\varepsilon_{yy} - \varepsilon_{yy0})), \quad (5) \\ T_{C,B}\left(\varepsilon_{xx}, \varepsilon_{yy}\right) &= T_C\left(0,0\right)\left(1 + g_B\left(\varepsilon_{xx} - \varepsilon_{xx0}\right)\right. \\ &\quad \left. + g_A(\varepsilon_{yy} - \varepsilon_{yy0})\right). \quad (6) \end{aligned}$$

In this paper, $T_C(0,0)$ is a constant equal to the critical temperature in both domains when $\varepsilon_{xx} = \varepsilon_{xx0}$ and $\varepsilon_{yy} = \varepsilon_{yy0}$. The parameter $g_A = (\partial T_{C,A}/\partial \varepsilon_{xx})_{\varepsilon_{yy}=0} = (\partial T_{C,B}/\partial \varepsilon_{yy})_{\varepsilon_{xx}=0}$ and $g_B = (\partial T_{C,B}/\partial \varepsilon_{xx})_{\varepsilon_{yy}=0} = (\partial T_{C,A}/\partial \varepsilon_{yy})_{\varepsilon_{xx}=0}$. g_A and g_B are the sensitivities of a (RE)BCO single crystal's T_C when there are *only* strains along the a- or b-axis respectively. The constants ε_{xx0} and ε_{yy0} are included to account for prestrains that can be induced in a (RE)BCO layer during a tape's manufacturing process and cool down, due to the mismatch in coefficients of thermal expansion between the different layers in the tape [6], [10], [29], [30]. In this paper we have chosen to set ε_{xx0} and ε_{yy0} to be equal to zero because, to first order, the prestrains induced during cool down are isotropic and we can expect that when there is no applied strain in either the x-direction or the y-direction that $T_{C,A} = T_{C,B} = T_C(0,0)$.

Table II gives the values of the free parameters used to generate the dotted and solid lines in Figs. 2–4. The parameters and their uncertainties were calculated using least-squares fitting. We set N equal to 18 from our measurements and a different value of A was allowed for each of the three sets of data (i.e., each combination of field angle and applied strain type). For the magnetic field and strain range of our experiments, N was not a function of strain. f, g_A and g_B were assumed to be independent of field angle (i.e., they were set as global free parameters) and p and q could take different values for different field angles. Better fits to all our data can be obtained by allowing p and q to be field dependent, but this adds additional complexity to the fitting procedure that does not help make the underlying science

TABLE II
PARAMETER VALUES FROM THE PARAMETERISATION OF THE $J_C(B, \varepsilon_{xx}, \varepsilon_{yy})$ DATA

Parameter	Value	
	$\theta = 90°$	$\theta = 0°$
f	0.49 ± 0.03	
g_A (K%$^{-1}$)	1.8 ± 0.1	
g_B (K%$^{-1}$)	-1.3 ± 0.1	
p	0.706 ± 0.006	0.674 ± 0.006
q	0.0 ± 0.2	5.8 ± 0.3
A_{DSI} (MAm^{-2}T$^{0.5}$K^{-2})	20.0 ± 0.5	23.2 ± 0.7
A_{DSII} (MAm^{-2}T$^{0.5}$K^{-2})	20.5 ± 0.5	23.2 ± 0.7
A_{DSIII} (MAm^{-2}T$^{0.5}$K^{-2})	21.5 ± 0.5	23.6 ± 0.7

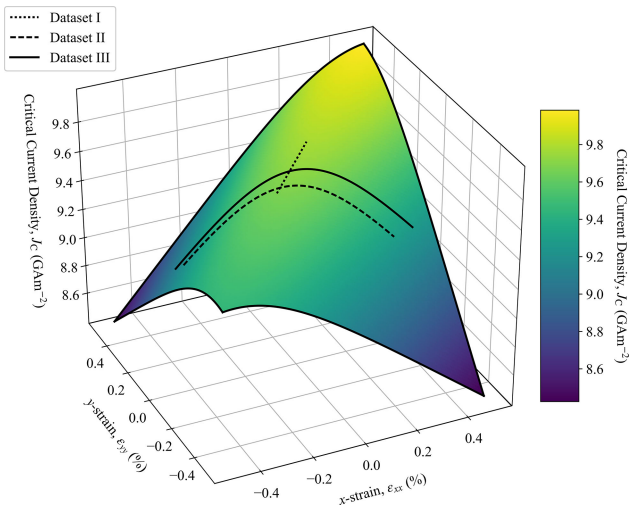

Fig. 5. The biaxial strain dependence of J_C for $T = 77$ K, $B = 0.5$ T and $\theta = 90°$. The surface and three lines are generated using the free parameters in Table II.

clearer. Fig. 5 shows a surface for $J_C(\varepsilon_{xx}, \varepsilon_{yy})$ generated from the free parameters derived in Table II and is shaped like a ridge. Three lines are plotted which correspond to each of the sets of data found in Figs. 2–4. The strain range for the J_C data in Fig. 2 maps a line on Fig. 5 that is parallel to the ridge and leads to the observed linear behavior for J_C. However, the J_C data in Fig. 3 and Fig. 4 correspond to a range of strains that pass over the ridge and lead to the parabolic behavior observed.

IV. DISCUSSION

The data in Figs. 2-4 demonstrate a change from linear behaviour in Fig. 2 to parabolic strain behavior in Fig. 3 and Fig. 4 for the same tape. A linear behaviour occurs in Fig. 2 because the $J_C's$ and $T_C's$ of the A- and B-domains both increase with increasing tensile $\varepsilon_{xx} = \varepsilon_{yy}$ strain. If $|g_A| > |g_B|$, then the tape's J_C increases with tensile $\varepsilon_{xx} = \varepsilon_{yy}$ strain and if $|g_A| < |g_B|$, the tape's J_C decreases with increasing tensile $\varepsilon_{xx} = \varepsilon_{yy}$ strain. Parabolic behaviour occurs in Figs. 3–4 because the J_C's of the A- and B-domains increase and decrease respectively with increasing tensile ε_{xx}. Hence, the J_C of the tape has a maximum value at which the sum of *E*-fields produced by the fractions of A- and B-domains are minimized for any transport current. The twin boundaries in the (RE)BCO layers of SuperPower's tapes are aligned with the [110] direction, however for other manufacturers such as Fujikura, the twin boundaries are aligned with the [100] direction [30]. The uniaxial strain dependencies of SuperPower's and Fujikura's tapes are parabolic and linear respectively [10], [31] and van der Laan *et al.* have shown that the in-plane strain dependence of J_C is anisotropic with respect to the direction of applied strain [5]. For the first time, we have been able to show both linear and parabolic strain behaviour on a single tape sample by applying strain in different directions with respect to the twin boundary orientation. Figs. 2–4 show that our theoretical description can produce the main features of the data but more work is needed to provide confidence in the theory described here.

The scatter on the J_C data in this paper is about $\sim$5% in Figs. 2–4. We attribute the scatter to an increase in contact resistance with (RE)BCO layers of the tape due to thermal cycling. The contact resistance increased during the course of this experiment but did not significantly affect $J_C(B, \varepsilon_{xx} = 0, \varepsilon_{yy} = 0)$. The tape and the probe were thermally cycled every time the applied strain was changed. This repeated thermal cycling risks damaging the sample and is very time-consuming. Future work will include biaxial strain measurements using equipment that can apply biaxial strains at low temperatures *in-situ*, as well as improving the strain range of the crossboard so the linear relationship in Fig. 2 can be verified for a larger strain range.

In order to obtain consistent fits to our data, we have allowed the scaling law fitting parameter A in (3) to vary between the three sets of strain data as well as between different field angles. More data are required to determine why this has been necessary. It is probably associated with plastic deformation in some components of the tape or the crossboard and is consistent with the relatively large variation in J_C of up to $\sim$10% at zero applied strain that we found throughout this experiment. For example, during the experiment, we noted that the strain state of the tape did not relax back to zero strain when we stopped applying stresses to the tape. We have also assumed that the single crystal variable strain data showing T_C is linear in strain can be extrapolated to tensile strains and over the relatively large range of strains measured in these experiments. This assumption needs independent verification.

Single crystal measurements from Welp *et al.* generated values of g_A and g_B that were positive and negative respectively and of roughly equal magnitude [28]. Our parameterisation gives g_A and g_B opposite signs, consistent with Welp, however the magnitude of our g_A and g_B values are approximately 30% different. Experiments on detwinned (RE)BCO tapes have also shown that g_A and g_B can have different magnitudes [27]. Indeed we expect some variability in these parameters from tapes because these tapes are loaded with APC's to increase J_C. However, these APC's will also strain the (RE)BCO material and introduce disorder.

V. CONCLUSION

We have completed J_C measurements on a single SuperPower SCS4050 APC tape sample at 77 K in fields up to 0.7 T using a

crossboard and have parameterised the results using our model. The model for $J_C(B, \varepsilon_{xx}, \varepsilon_{yy})$ treats the (RE)BCO layer as a 1D chain of A- and B- domains that have their *a*- and *b*-axes aligned with the length of the tape respectively. We have shown that the fraction of A-domains in the (RE)BCO layer is roughly the same as the B-domains (i.e., f is 0.49) and that the strain sensitivities of the T_C's of both domain types have values of 1.8 $K\%^{-1}$ for strains along the *a*-axis and -1.3 $K\%^{-1}$ for strains along the *b*-axis. By using biaxial strain measurements, we have observed and explained for the first time, a change between linear strain behavior for J_C and parabolic strain behaviour for J_C in the *same* tape. In the future, we aim to investigate parabolic and linear strain behaviour on tape samples from other manufacturers which have different twin boundary orientations.

ACKNOWLEDGMENT

The authors would like to thank P. Branch and T. Hynes for useful discussions, and S. Lishman in the Durham Mechanical Workshop for helping to design the crossboard. Data are available at: http://dx.doi.org/10.15128/r1z890rt249 and associated materials are at: http://dro.dur.ac.uk/.

REFERENCES

[1] J. D. Weiss, T. Mulder, H. J. ten Kate, and D. C. Van der Laan, "Introduction of CORC wires: Highly flexible, round high-temperature superconducting wires for magnet and power transmission applications," *Supercond. Sci. Technol.*, vol. 30, no. 1, 2016, Art. no. 014002.

[2] P. Bruzzone *et al.*, "High temperature superconductors for fusion magnets," *Nucl. Fusion*, vol. 58, no. 10, 2018, Art. no. 103001.

[3] J. S. Murtomaki *et al.*, "Investigation of REBCO Roebel cable irreversible critical current degradation under transverse pressure," *IEEE Trans. Appl. Supercond.*, vol. 28, no. 4, Jun. 2018, Art. no. 4802506.

[4] V. A. Anvar *et al.*, "Bending of CORC cables and wires: Finite element parametric study and experimental validation," *Supercond. Sci. Technol.*, vol. 31, no. 11, 2018, Art. no. 115006.

[5] D. C. van der Laan *et al.*, "Anisotropic in-plane reversible strain effect in $Y_{0.5}Gd_{0.5}Ba_2Cu_3O_{7-\delta}$ coated conductors," *Supercond. Sci. Technol.*, vol. 24, no. 11, 2011, Art. no. 115010.

[6] P. Branch, Y. Tsui, K. Osamura, and D. P. Hampshire, "Multimodal strain dependence of the critical parameters in high-field technological superconductors," *Supercond. Sci. Technol.*, to be published.

[7] P. Sunwong, J. S. Higgins, Y. Tsui, M. J. Raine, and D. P. Hampshire, "The critical current density of grain boundary channels in polycrystalline HTS and LTS superconductors in magnetic fields," *Supercond. Sci. Technol.*, vol. 26, no. 9, 2013, Art. no. 095006.

[8] D. C. van der Laan, J. W. Ekin, J. F. Douglas, C. C. Clickner, T. C. Stauffer, and L. F. Goodrich, "Effect of strain, magnetic field and field angle on the critical current density of $YBa_2Cu_3O_{7-\delta}$ coated conductors," *Supercond. Sci. Technol.*, vol. 23, no. 7, 2010, Art. no. 072001.

[9] H. S. Shin, M. J. Dedicatoria, A. Gorospe, H. Oguro, and S. Awaji, "I_c response with high magnetic field, low temperature, and uniaxial strain in REBCO coated conductor tapes," *IEEE Trans. Appl. Supercond.*, vol. 26, no. 4, Jun. 2016, Art. no. 8401504.

[10] K. Osamura, S. Machiya, and D. P. Hampshire, "Mechanism for the uniaxial strain dependence of the critical current in practical REBCO tapes," *Supercond. Sci. Technol.*, vol. 29, no. 6, 2016, Art. no. 065019.

[11] C. Barth, G. Mondonico, and C. Senatore, "Electro-mechanical properties of REBCO coated conductors from various industrial manufacturers at 77 K, self-field and 4.2 K, 19 T," *Supercond. Sci. Technol.*, vol. 28, no. 4, 2015, Art. no. 045011.

[12] C. Senatore, C. Barth, M. Bonura, M. Kulich, and G. Mondonico, "Field and temperature scaling of the critical current density in commercial RE-BCO coated conductors," *Supercond. Sci. Technol.*, vol. 29, no. 1, 2016, Art. no. 014002.

[13] K. Ilin *et al.*, "Experiments and FE modeling of stress-strain state in ReBCO tape under tensile, torsional and transverse load," *Supercond. Sci. Technol.*, vol. 28, no. 5, 2015, Art. no. 055006.

[14] M. Takayasu, J. Minervini, and L. Bromberg, "Torsion strain effects on critical currents of HTS superconducting tapes," *AIP Conf. Proc.*, vol. 1219, no. 337, pp. 337–344, 2010.

[15] D. C. van der Laan, D. C. McRae, and J. D. Weiss, "Effect of transverse compressive monotonic and cyclic loading on the performance of superconducting CORC cables and wires," *Supercond. Sci. Technol.*, vol. 32, no. 1, 2018, Art. no. 015002.

[16] J. R. Greenwood, E. Surrey, and D. P. Hampshire, "Biaxial strain measurements of Jc on a (RE)BCO coated conductor," *IEEE Trans. Appl. Supercond.*, vol. 28, no. 4, Jun. 2018, Art. no. 8400705.

[17] W. H. Fietz, K. P. Weiss, and S. I. Schlachter, "Influence of intrinsic strain on T_c and critical current of high-T_c superconductors," *Supercond. Sci. Technol.*, vol. 18, no. 12, pp. S332–S337, 2005.

[18] HBM, "XY T rosettes with 2 measuring grids for analyzing biaxial stress states with known principal directions," 2018. [Online]. Available: https://www.hbm.com/en/3443/xy-t-rosettes-with-measuring-grids-for-analyzing-biaxial-stress/. Accessed: Dec. 10, 2018.

[19] S. A. Keys and D. P. Hampshire, "A scaling law for the criticalurrent density of weakly and strongly-coupled superconductors, used to parameterise data from a technological Nb_3Sn strand," *Supercond. Sci. Technol.*, vol. 16, pp. 1097–1108, 2003.

[20] D. M. J. Taylor and D. P. Hampshire, "The scaling law for the strain dependence of the critical current density in Nb_3Sn superconducting wires," *Supercond. Sci. Technol.*, vol. 18, pp. S241–S252, 2005.

[21] Y. Tsui and D. P. Hampshire, "Critical current scaling and the pivot-point in Nb_3Sn strands," *Supercond. Sci. Technol.*, vol. 25, no. 5, 2012, Art. no. 054008.

[22] X. F. Lu and D. P. Hampshire, "The magnetic field, temperature and strain dependence of the critical current of a Nb_3Sn strand using a six free-parameter scaling law," *IEEE Trans. Appl. Supercond.*, vol. v19, no. 3, pp. 2619–2623, Jun. 2009.

[23] X. F. Lu, D. M. J. Taylor, and D. P. Hampshire, "Critical current scaling laws for advanced Nb_3Sn superconducting strands for fusion applications with six free parameters," *Supercond. Sci. Technol.*, vol. 21, no. 10, 2008, Art. no. 105016.

[24] E. J. Kramer, "Scaling laws for flux pinning in hard superconductors," *J. Appl. Phys.*, vol. 44, no. 3, pp. 1360–1370, 1973.

[25] S. A. Keys, N. Koizumi, and D. P. Hampshire, "The strain and temperature scaling law for the critical current density of a jelly-roll Nb_3Al strand in high magnetic fields," *Supercond. Sci. Technol.*, vol. 15, pp. 991–1010, 2002.

[26] T. Sekitani, N. Miura, S. Ikeda, Y. H. Matsuda, and Y. Shiohara, "Upper critical field for optimally-doped $YBa_2Cu_3O_{7-\delta}$," *Physica B*, vol. 346–347, pp. 319–324, 2004.

[27] S. Awaji, T. Suzuki, H. Oguro, K. Watanabe, and K. Matsumoto, "Strain-controlled critical temperature in $REBa_2Cu_3O_y$-coated conductors," *Sci. Rep.*, vol. 5, 2015, Art. no. 11156.

[28] U. Welp, M. Grimsditch, S. Fleshler, W. Nessler, J. Downey, and G. W. Crabtree, "Effect of uniaxial stress on the superconducting transition in $YBa_2Cu_3O_7$," *Phys. Rev. Lett.*, vol. 69, no. 14, pp. 2130–2133, 1992.

[29] K. Osamura, S. Machiya, Y. Tsuchiya, and H. Suzuki, "Force free strain exerted on a YBCO layer at 77 K in surround Cu stabilized YBCO coated conductors," *Supercond. Sci. Technol.*, vol. 23, no. 4, 2010, Art. no. 045020.

[30] K. Osamura *et al.*, "Microtwin structure and its influence on the mechanical properties of REBCO coated conductors," *IEEE Trans. Appl. Supercond.*, vol. 22, no. 1, Feb. 2012, Art. no. 8400809.

[31] M. Sugano *et al.*, "The effect of the 2D internal strain state on the critical current in GdBCO coated conductors," *Supercond. Sci. Technol.*, vol. 25, no. 5, 2012, Art. no. 054014.